

Effects of density gradients on measurements of the decay rate of spontaneous density fluctuations in fluids near the critical point*

Dae M. Kim, Donald L. Henry, and Riki Kobayashi

Department of Electrical Engineering and Department of Chemical Engineering, Rice University, Houston, Texas 77001

(Received 11 April 1974)

Gravitationally induced, anomalous density gradients in a fluid near the critical point are shown to have significant effects on light-scattering measurements of the decay rate of density fluctuations along the critical isochore. We have calculated the height dependence of the decay rate for xenon and carbon dioxide using a parametric equation of state and both the mode-mode coupling and the decoupled-mode theories of critical-point dynamics, and have found that the minimum in the decay rate, which does not always occur at the height of the critical isochore, can be several percent lower than the value at the critical isochore. In addition, the density gradient across the diameter of the incident light beam is shown to give rise to a measured decay rate significantly different from the value at the center of the beam, particularly at small scattering angles, under some typical experimental conditions.

I. INTRODUCTION

The spectrum of laser light scattered from a fluid contains a quasielastic component, called the Rayleigh line, centered on the frequency of the incident laser light, whose width is the decay rate (Γ) of spontaneous density fluctuations.¹ Near the critical point the isothermal compressibility (K_T) diverges, inducing a vertical density gradient in Earth's gravitational field, and the decay rate then depends on the height in the sample. The value of the decay rate at the critical isochore has generally been obtained by assuming (a) that Γ as a function of height at a fixed temperature and scattering angle is minimum at the critical isochore and (b) that the density gradient across the width of the laser beam has a negligible effect on the measurement of Γ . In this paper we carefully examine the validity of these underlying assumptions, since in fact the density gradient is most pronounced in the region of the critical isochore, and the detailed behavior of Γ as a function of height in the sample in this region has not previously been analyzed explicitly.

Furthermore, a recent analysis of experimental Rayleigh linewidth data by Swinney and Henry indicated that more data are needed in a region very close to the critical point in order to test the results of two theories of dynamics near a critical point.² These theories, the mode-mode coupling³⁻⁵ and the decoupled-mode^{6,7} theories, predict slightly different values for the decay rate very close to the critical point. It is therefore important to consider possible complications in the interpretation of experimental data in that region.

In Sec. II we briefly consider the time autocorrelation function of the electric field scattered from a fluid. The method used for determining the

height dependence of the decay rate and other thermodynamic quantities that appear in the autocorrelation function is described in Sec. III; in particular, the detailed behavior of Γ as a function of height in the sample near the critical isochore as predicted by both the mode-mode coupling theory and the decoupled-mode theory is discussed. In Sec. IV we analyze in detail the effects of a finite density gradient across the laser beam diameter on the measurement of Γ . The results of specific calculations for xenon and carbon dioxide are also presented. In Sec. V we discuss the significance of our analysis.

II. TIME AUTOCORRELATION FUNCTION OF SCATTERED FIELD

The geometry of a light scattering experiment is shown in Fig. 1. Laser light having the carrier frequency ω_0 and wave vector \vec{k}_0 is scattered from the sample at an angle θ with a resulting wave vector \vec{k}_s . The magnitude of the momentum transfer vector, $\vec{q} \equiv \vec{k}_0 - \vec{k}_s$ is then given to a good approximation by $q = (4\pi/\lambda) \sin \frac{1}{2}\theta$, λ being the wavelength of the light in the sample. The time-correlation function of the scattered electric field,^{1,8}

$$C_E(t) \equiv \langle E_s^*(0)E_s(t) \rangle, \quad (1)$$

is related to the spontaneous decay rate Γ of the q th component of the density fluctuation, ρ_q , by¹

$$C_E(t) \propto \langle |\rho_q|^2 \rangle e^{-\Gamma t}. \quad (2)$$

By using the Ornstein-Zernike theory⁹ $\langle |\rho_q|^2 \rangle$ can be expressed in terms of the sample density ρ , the compressibility K_T , and the long-range correlation length ξ , as

$$\langle |\rho_q|^2 \rangle = \rho^2 K_T / (1 + q^2 \xi^2). \quad (3)$$

K_T can in turn be related to ξ by the compressibility theorem of statistical theory¹⁰:

$$\rho \bar{K}_T(\rho) / \rho_c K_T(\rho_c) = [\xi(\rho) / \xi(\rho_c)]^2, \quad (4)$$

ρ_c being the critical density. Thus Eq. (2) can be rewritten as

$$C_E(t) = C \rho \xi^2 e^{-\Gamma t} / (1 + q^2 \xi^2), \quad (5)$$

where the proportionality constant C is independent of density. Equation (5) will be used in the calculation of the density dependence of the time-correlation function.

III. HEIGHT DEPENDENCE OF THE DECAY RATE

To determine the height dependence of the decay rate, it is necessary to have an equation of state for the fluid. Recently Schofield,¹¹ and Ho and Litster¹² introduced a general parametric representation of scaling laws, and the ensuing equation of state, which we adopt here, has been shown to fit experimental data to high accuracy for a number of fluids.¹³

In the parametric representation of the equation of state, a point in the (ρ, T) plane is specified by the two independent variables r and θ . The linear model of the equation of state is described by

$$\epsilon \equiv (T - T_c) / T_c = (1 - b^2 \theta^2) r, \quad (6a)$$

$$\Delta \rho \equiv (\rho - \rho_c) / \rho_c = k \theta r^b, \quad (6b)$$

$$\Delta \mu \equiv [\mu(\rho, T) - \mu(\rho_c, T)] \rho_c / P_c = a \theta (1 - \theta^2) r^{\beta \delta}. \quad (6c)$$

Here μ and P denote, respectively, the chemical potential and the pressure, and the subscript c refers to values at the critical point. As shown in Fig. 2, the two-phase region is bounded by $\theta = \pm 1$, the critical isotherm is given by $\theta = \pm b^{-1}$, and the critical isochore by $\theta = 0$ for $T > T_c$. The constants

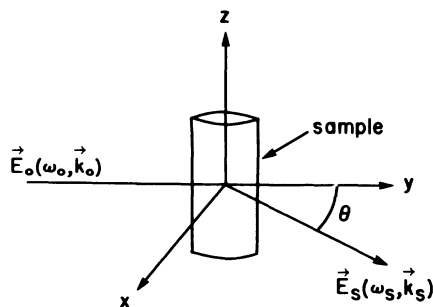


FIG. 1. Schematic diagram of the light-scattering geometry. The incident field \vec{E}_0 propagates along the y direction with wave vector \vec{k}_0 and frequency ω_0 and is scattered from the sample at an angle θ with wave vector \vec{k}_s and ω_s . The z axis is taken parallel to Earth's gravitational field.

$a, b, k, \beta,$ and δ are determined from a fit to experimental data for the fluid under consideration.

The theoretical prediction for the decay rate Γ can be deduced from the procedure described in detail by Swinney and Henry,² which we briefly outline here. Γ is assumed to be the sum of a background (i.e., nonanomalous) part and a critical part:

$$\Gamma = \lambda^B q^2 (1 + q^2 \xi^2) / \rho c_p + \Gamma^c, \quad (7)$$

where λ^B is the background thermal conductivity, which is calculated from thermal conductivity data obtained away from the critical point.¹⁴ The specific heat at constant pressure, c_p , is related to the isothermal compressibility and the specific heat at constant volume, c_v , through the thermodynamic relation

$$\rho c_p = \rho c_v + T \left(\frac{\partial P}{\partial T} \right)_\rho^2 K_T. \quad (8)$$

Very near the critical point, only the second term in Eq. (8) is significant, and $(\partial P / \partial T)_\rho$ is only weakly density dependent. Furthermore, the background contribution to the decay rate is at most only a few percent of the total decay rate for the temperature ranges considered here.

There are two theories for the critical part Γ^c : (a) the mode-mode coupling theory³⁻⁵ and (b) the decoupled-mode theory.^{6,7} The mode-mode coupling expression for Γ^c is

$$\Gamma^c = k_B T K_0(q\xi) R(q\xi) C(q\xi) / 6\pi \eta_s \xi^3, \quad (9a)$$

where k_B is the Boltzmann constant and η_s is the shear viscosity; $R(q, \xi)$ and $C(q\xi)$ are numerically evaluated factors which incorporate various refine-

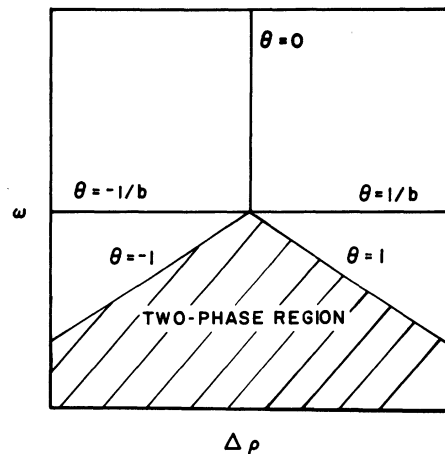


FIG. 2. Schematic representation of the $(\epsilon, \Delta \rho)$ plane in terms of the parametric variables (r, θ) . The two-phase region is bounded by $\theta = 1$ (liquid) and $\theta = -1$ (vapor); the critical isochore is specified by $\theta = 0$, and the critical isotherm by $\theta = \pm 1/b$.

ments to the mode-mode coupling theory, and $K_0(x)$ is given by

$$K_0(x) = \frac{3}{4}[1 + x^2 + (x^3 - 1/x) \arctan(x)]. \quad (9b)$$

Additionally, the shear viscosity η_s can be treated by decomposing it into a background part η_s^B and a critical part η_s^c , with η_s^c given theoretically by

$$\eta_s^c = (8\bar{\eta}/15\pi^2) \ln(q_D \xi), \quad (9c)$$

where $\bar{\eta}$ and q_D are parameters determined from a fit to experimental data.

The decoupled-mode theory gives

$$\Gamma^c = k_B T K_0(q\xi) C(q\xi) / 6\pi \eta_s^{\text{eff}} \xi^3, \quad (10a)$$

where the effective shear viscosity η_s^{eff} is defined by

$$\eta_s^{\text{eff}} = \eta_s^B \left\{ 1 + (8\bar{\eta}/15\pi^2 \eta_s^B) [\ln q_D \xi - \frac{1}{2} \ln(1 + q^2 \xi^2) + \tau(q\xi)] \right\}. \quad (10b)$$

$K_0(q\xi)$ and $C(q\xi)$ are the same functions that appear in Eq. (9a), and $\tau(q\xi)$ is a function which has been determined numerically. The parameters $\bar{\eta}$ and q_D are the same parameters appearing in Eq. (9c).

These two theories for Γ^c differ significantly only in a region very near the critical point (i.e., for $q\xi > 1$), where the difference is a few percent. Hence in order to test the two theories it is important to obtain accurate decay-rate data in a region where density gradients will be most pronounced.

The density dependence of the decay rate is determined by the density dependence of the correlation length ξ (and to a lesser extent the background shear viscosity η^B), which can be found from Eq. (4) with K_T expressed in terms of the parametric equation of state as

$$K_T = \frac{k}{P_c a (1 + k\theta r^B)^2} \left(1 + \frac{\theta^2 (2\beta\delta - 3)}{1 - 2\beta} \right)^{-1} r^{-\gamma}. \quad (11)$$

In our discussion thus far, all the quantities in Eq. (5) have been related to the density through the equation of state. Height dependence is introduced through the relation

$$z - z_c = -(1/g) [\mu(\rho, T) - \mu(\rho_c, T)], \quad (12)$$

where g is the acceleration of gravity and z_c is the height corresponding to the critical density.

Since light-scattering experiments are usually performed at some fixed temperature T , the two independent variables r and θ which appear in the equation of state are constrained by Eq. (6a). Consequently, by combining Eqs. (6) through (12) one can express explicitly all the quantities appearing in Eq. (5) in terms of either the sample height z or one of the variables r or θ .

We now illustrate the substantial height dependence of the density, the correlation length and

the decay rate using Eqs. (6)–(12) for the specific cases of xenon and carbon dioxide. Values for the constants appearing in the equation of state were obtained from Hohenberg and Barmatz¹⁵ (see their Table I), and the parameters needed for calculating the decay rate were obtained from Swinney and Henry² (see their Tables III and VII). Most of the results discussed in the remainder of this section will be confined to carbon dioxide, since very similar results were obtained for xenon.

The density as a function of height z calculated with the parametric equation of state is shown in Fig. 3 for CO₂ at four temperatures ($T - T_c \equiv \Delta T = 0.001, 0.01, 0.1, \text{ and } 1 \text{ K}$). Note in particular that at $\Delta T = 0.001 \text{ K}$ the variation in density across a 0.02-cm interval (a typical value for the diameter of a focused laser beam) centered at the height corresponding to the critical density is about 3%. (For xenon, this variation in density is 8%). Clearly, the effects of such a large density gradient across a laser beam must be examined carefully.

Figure 4 shows the correlation length $\xi(z)/\xi(z_c)$ [see Eqs. (4) and (11)] as a function of height for CO₂. Note that at $\Delta T = 0.001 \text{ K}$, the correlation length at $z - z_c = 0.01 \text{ cm}$ has decreased to about 60% of its value at z_c .

Figure 5 shows the decay rate $\Gamma(z)/\Gamma(z_c)$ as a function of height at the scattering angle $\theta = 90^\circ$, and at three temperatures for CO₂ with Γ^c calculated from the mode-mode coupling theory. Clearly, the decay rate varies quite rapidly over

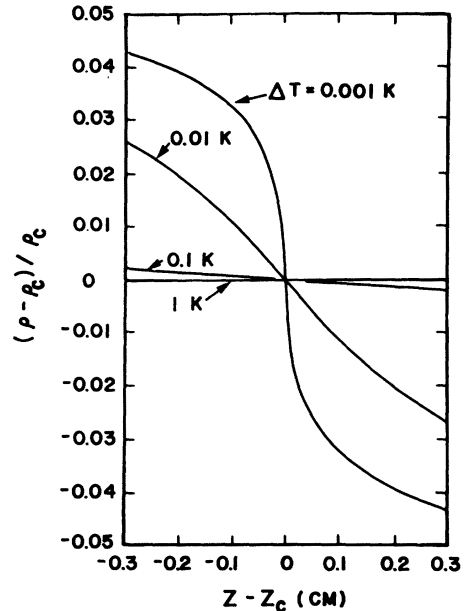


FIG. 3. Density of CO₂ as a function of height at four isotherms ($\Delta T = 0.001, 0.01, 0.1 \text{ K}$) as determined from the parametric equation of state.

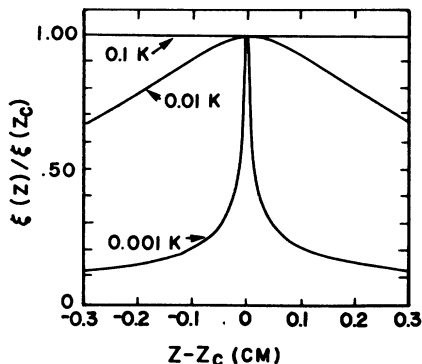


FIG. 4. Relative correlation length $\xi(z)/\xi(z_c)$ vs height for CO_2 at three different temperatures ($\Delta T=0.1, 0.01,$ and 0.001 K).

a short height interval for small ΔT . Furthermore, we obtain the unexpected result that the absolute minimum in Γ as a function of z at $\Delta T=0.001$ K does *not* occur at the critical isochore but is 6% smaller than $\Gamma(z_c)$. Figure 6 shows $\Gamma(z)$ over a smaller range in z and ΔT , and we see that the minimum in Γ ranges from 1.8% less than $\Gamma(z_c)$ for $\Delta T=0.003$ K to 5.8% for $\Delta T=0.0005$ K, and the location of the minimum ranges from $\Delta z \equiv z - z_c = -0.027$ cm for $\Delta T=0.003$ K to -0.020 cm for $\Delta T=0.0005$ K. Table I lists the values of the minimum in $\Gamma(z)/\Gamma(z_c)$ and the corresponding values of Δz for both xenon and CO_2 for several angles and tem-

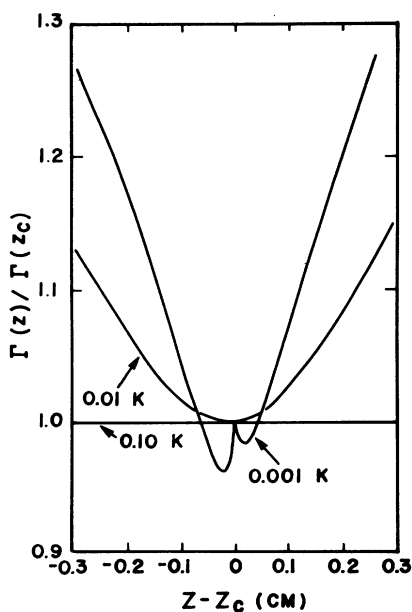


FIG. 5. Decay rate $\Gamma(z)/\Gamma(z_c)$ vs Δz for CO_2 at $\theta=90^\circ$ and for three temperatures ($\Delta T=0.001, 0.01,$ and 0.1 K) with Γ^c calculated from the mode-mode coupling theory. $\Delta T=0.001$ K, the minimum in $\Gamma(z)$ does not occur at the critical isochore (i.e., $z=z_c$).

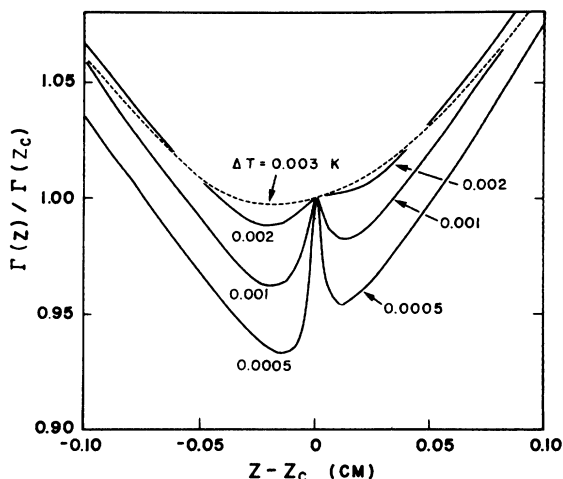


FIG. 6. $\Gamma(z)/\Gamma(z_c)$ for CO_2 as a function of z over a 0.2-cm interval for four temperatures, with the critical part of the decay rate calculated from the mode-mode coupling theory. At these temperatures the (absolute) minimum in $\Gamma(z)$ occurs below the height of the critical isochore. The difference in the values of the two minima about z_c is due to the weak density dependence of the background shear viscosity.

peratures. For angles less than about 30° , the minimum values are located at $z=z_c$. For both fluids the minimum value of Γ can be as much as 6% less than the value at critical isochore.

The above behavior of $\Gamma(z)$ can be explained by considering $q\xi$ as a function of z and Γ as a function of $q\xi$. As indicated in Fig. 4, $q\xi(z)$ is maximum at $z=z_c$ for all temperatures and angles. Curve (a) in Fig. 7 is a plot of Γ vs $q\xi$ for CO_2 at

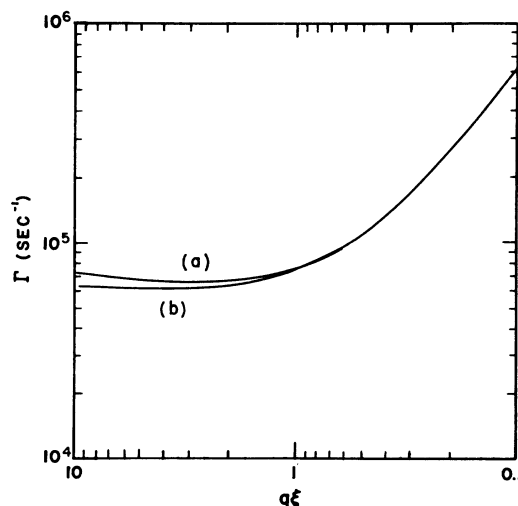


FIG. 7. Γ as a function of $q\xi$ for CO_2 as given by (a) the mode-mode coupling theory and (b) the decoupled-mode theory (for $\theta=90^\circ$). These curves include the background part of the decay rate.

TABLE I. The minimum value of $\Gamma(z)/\Gamma(z_c)$ and the corresponding height $\Delta z \equiv z - z_c$ for (a) CO_2 and (b) Xe at several temperatures and scattering angles with Γ calculated from the mode-mode coupling and the decoupled-mode theories.

ΔT (K)	θ (deg)	Mode-mode coupling		Decoupled-mode	
		$\Gamma(z)/\Gamma(z_c)$ minimum	Δz at min. (cm)	$\Gamma(z)/\Gamma(z_c)$ minimum	Δz at min. (cm)
(a) CO_2					
0.0005	180	0.918	-0.017	0.982	-0.008
	145	0.919	-0.017	0.983	-0.008
0.001	90	0.932	-0.017	0.987	-0.005
	60	0.955	-0.008	0.994	-0.002
	180	0.940	-0.035	0.989	-0.010
	145	0.943	-0.035	0.989	-0.010
0.002	90	0.962	-0.020	0.994	-0.007
	60	0.982	-0.008	0.998	-0.003
	180	0.969	-0.041	0.995	-0.016
	145	0.972	-0.041	0.996	-0.013
0.003	90	0.987	-0.019	0.998	-0.007
	60	0.997	-0.007	0.999	-0.004
	180	0.984	-0.043	0.997	-0.015
	145	0.986	-0.043	0.997	-0.015
0.0005	180	0.908	-0.006	0.984	-0.002
	145	0.908	-0.006	0.983	-0.002
	90	0.914	-0.006	0.985	-0.002
	60	0.935	-0.002	0.990	-0.001
0.001	180	0.923	-0.014	0.986	-0.004
	145	0.925	-0.014	0.987	-0.004
	90	0.943	-0.007	0.992	-0.002
	60	0.967	-0.004	0.997	-0.001
0.002	180	0.952	-0.017	0.993	-0.006
	145	0.955	-0.017	0.994	-0.005
	90	0.973	-0.008	0.997	-0.003
	60	0.991	-0.004	0.999	-0.001
0.003	180	0.969	-0.019	0.996	-0.007
	145	0.971	-0.019	0.997	-0.006
	90	0.987	-0.009	0.998	-0.003
	60	0.998	-0.004	0.999	-0.002

$\Delta T = 0.001$ K and $\theta = 90^\circ$ with Γ calculated from the mode-mode coupling theory. In the region $q\xi \geq 3.5$ the decay rate *decreases* with decreasing $q\xi$ until a minimum is reached at $q\xi \approx 3.5$. That is, $\Gamma(q\xi = 3.5)/\Gamma(q\xi > 3.5) < 1$, and the minimum in $\Gamma(z)$ will occur at the value of $|\Delta z|$ corresponding to $q\xi \approx 3.5$. Because of the density dependence of the background shear viscosity, the minimum in $\Gamma(z)$ for $\Delta z > 0$ is not as small as for $\Delta z < 0$. At angles less than about 35° , $q\xi(z_c)$ is less than 3.5 (for $\Delta T = 0.001$ K) so that the minimum in $\Gamma(z)$ will occur at $\Delta z = 0$. It should be emphasized that the *magnitude* of the minimum in $\Gamma(z)$ is independent of the model used for the equation of state but depends only on the theory used for calculating Γ^c . Only the *height* at which the minimum occurs depends

on the equation of state.

Curve (b) in Fig. 7 shows Γ as a function of $q\xi$ (at $\theta = 90^\circ$) with Γ^c calculated from the decoupled-mode theory. The slope of Γ as a function of $q\xi$ for $q\xi > 3$ is not as steep as in curve (a), so that the minimum value of $\Gamma(z)$ predicted by the decoupled-mode theory will be closer to $\Gamma(z_c)$ than those predicted by the mode-mode coupling theory (see Table I).

The decay rate shown in Fig. 7 consists of both background and critical parts. The background Γ^B , however, is only a small fraction of the total decay rate in the region $q\xi > 1$; e.g., $\Gamma^B/\Gamma \approx 8\%$ at $q\xi = 1$ and 6% at $q\xi = 10$. Moreover, the same values for Γ^B are used in curves (a) and (b). Hence the significant difference between these curves is

due to the difference between the two theories for the critical part Γ^c .

The predictions of the two theories for $\Gamma(z)$ are compared on an absolute basis in Fig. 8, which shows $\Gamma(z)$ for (a) the mode-mode coupling theory and (b) the decoupled-mode theory for CO_2 at $\theta = 90^\circ$ and $\Delta T = 0.001$ K. The results for $\Gamma(z_c)$ differ by 10.6%, but the minimum values of $\Gamma(z)$ differ by 7.5% (and are located at slightly different heights).

As a check on our procedure for determining $\Gamma(z)$, we have compared our calculated values of $\Gamma(z)$ for xenon with those obtained by Lim¹⁶ (see Fig. 2 of Ref. 2). Figure 9 shows the decay rate as a function of z at $\Delta T = 0.018$ K and $\theta = 90^\circ$; the circles represent the experimental data and the solid line represents the calculated values. The agreement is very good at a temperature which is far enough from T_c that the finite-beam diameter effect is negligible (as will be shown in the following section) yet close enough for a density gradient to be present. This agreement lends confidence to our procedure.

We have shown that the assumption that the minimum in the decay rate as a function of height in the fluid occurs at the critical isochore is not valid at temperatures very near the critical point ($\Delta T < 0.003$ K) and at scattering angles greater than about 30° . In the next section we examine the assumption that the density gradient across the diameter of the laser beam has a negligible effect on the measurement of the decay rate.

IV. SPATIALLY AVERAGED TIME AUTOCORRELATION FUNCTIONS

We consider in this section the effects of a density gradient across the width of a laser beam on the measurement of the decay rate. Consider a laser

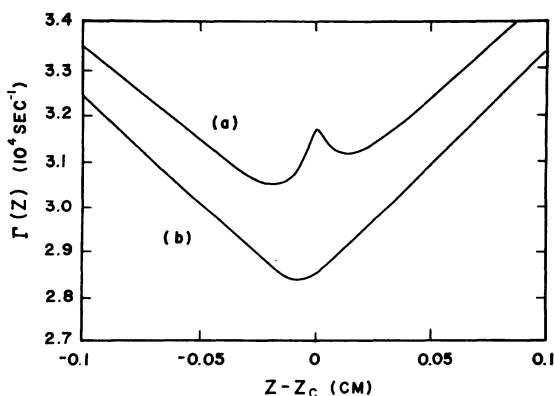


FIG. 8. Absolute value of Γ vs z for CO_2 at $\theta = 90^\circ$ and $\Delta T = 0.001$ K as given by (a) the mode-mode coupling theory and (b) the decoupled-mode theory. In both cases the minimum in $\Gamma(z)$ occurs below the critical isochore.

field excited in the Gaussian transverse mode, incident on the sample along the y direction. The intensity profile across the beam diameter D is given by

$$I(x, z) = I_0(2/D\pi^{1/2})^2 \exp\{-[(2/D)^2(x^2 + z^2)]\}, \quad (13)$$

where the z direction is taken parallel to the sample height (see Fig. 1).

As has been discussed in detail in the previous section, the quantities on which the field time autocorrelation function depends [see Eq. (5)] vary appreciably over a small but finite laser beam diameter D . Hence the measured time autocorrelation function of the scattered light should be averaged over the sample height:

$$\langle S(q, t) \rangle_z = C \int_{-\infty}^{\infty} W(z) e^{-\Gamma(z)t} dz, \quad (14a)$$

where the weighting factor $W(z)$ is the product of the incident-beam intensity profile and the intensity of the scattered light:

$$W(z) = \frac{(2I_0/D\pi^{1/2})\rho(z)\xi^2(z)}{[1 + q^2\xi^2(z)] \exp[2(z - z_0)/D]^2}. \quad (14b)$$

The midpoint of the laser beam is designated by z_0 and the x dependence of the beam intensity has been integrated out. The effects of refraction of light in the sample scattering volume are small and are neglected. Finite collection-aperture effects have also been neglected; Czwozniak and Jones have shown that such effects should be small for the Rayleigh component.¹⁷

We next turn to the specific calculation of Eq. (14). Although one can express the various quantities appearing in the integrand of Eq. (14) in terms of z , the algebra becomes quite complicated. Instead, one can circumvent this complexity by

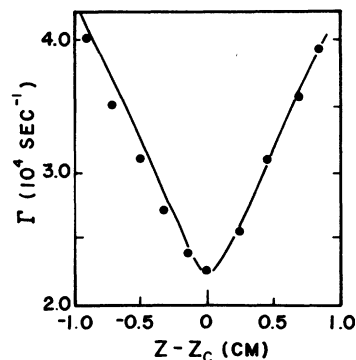


FIG. 9. Γ as a function of z for xenon at $\theta = 90^\circ$ and $\Delta T = 0.018$ K. The curve represents the calculated height dependence, and the circles are the values measured by Lim (Ref. 16). At this angle and temperature both the mode-mode coupling and the decoupled-mode theories give the same results for Γ .

transforming the integration from the sample height z to the variable θ . Thus, we can rewrite Eq. (14) as

$$\langle S(q, t) \rangle_z = C' \int_{-1/b}^{1/b} d\theta W'(\theta) e^{-\Gamma(\theta)t} \quad (15a)$$

where

$$W'(\theta) = \left(\frac{\partial z}{\partial \theta} \right)_T W[z(\theta)], \quad (15b)$$

and

$$z(\theta) - z(\theta_0) = -(P_c/\rho_c g) a \theta (1 - \theta^2) (1 - b^2 \theta^2)^{-\beta \delta} \epsilon^{\beta \delta} \quad (16)$$

The weighting function $W'(\theta)$ differs from $W(z)$ by the "scaling factor" $(\partial z/\partial \theta)_T$, and θ_0 corresponds to the midpoint z_0 of the laser beam. In this θ space, the range of integration is from $-1/b$ to $1/b$, as can be seen from Eq. (16).

As is clear from Fig. 5, the spread in the decay rate associated with the density gradient across a laser beam diameter is small, compared with the absolute value at the beam center, Γ_0 , i.e.,

$$\Delta\Gamma/\Gamma_0 \equiv [\Gamma(\theta) - \Gamma_0]/\Gamma_0 \ll 1. \quad (17)$$

By using Eq. (17), we can recast Eq. (15) in the following convenient form:

$$\langle S(q, t) \rangle_z = S_0 \left(1 + \sum_{n=1}^{\infty} \frac{(-1)^n \langle V_n \rangle (\Gamma_0 t)^n}{n!} \right) e^{-\Gamma_0 t}, \quad (18)$$

where the moments of the fractional spread in decay rate, i.e. $\Delta\Gamma/\Gamma_0$, are given by

$$\langle V_n \rangle \equiv \int_{-1/b}^{1/b} d\theta W'(\theta) (\Delta\Gamma/\Gamma_0)^n / \int_{-1/b}^{1/b} d\theta W'(\theta). \quad (19)$$

Equation (18) gives the practical relationship between the measured autocorrelation of scattered light and the decay rate of density-density fluctuations in the fluid. In the limit of either an infinitesimal laser beam diameter or a negligible density gradient in the sample, for which $\langle V_n \rangle = 0$ the decay constant of the time autocorrelation function, $\langle S(q, t) \rangle_z$ of the scattered field is equal to the decay rate of the fluid. However, in the presence of a large density gradient at some temperature ϵ , the laser beam may sample substantially different values of Γ across its beam diameter with different weighting factors. In this case one should exercise caution in deducing the decay rate from $\langle S(q, t) \rangle_z$. The case of particular practical interest corresponds to the situation in which only the first-order moment $\langle V_1 \rangle$ modifies significantly the overall time dependence of $\langle S(q, t) \rangle_z$. Assuming $\langle V_1 \rangle \ll 1$, the effective decay rate γ_m defined by

$$\langle S(q, t) \rangle_z \approx S_0 e^{-\gamma_m t}$$

is related to the decay rate Γ_0 at the midpoint of the beam by

$$\gamma_m = \Gamma_0 (1 + \langle V_1 \rangle). \quad (20)$$

The true decay rate of the sample density fluctuations at the critical isochore can be obtained from Eq. (20) by measuring the exponential decay constant γ_m of the time autocorrelation function of the scattered field and by correcting for the spatial averaging effect, namely $\langle V_1 \rangle$, provided the beam midpoint z_0 coincides with the height z_c of the critical isochore. The first-order moment $\langle V_1 \rangle$ then represents the fractional departure of the measured decay rate from the true value Γ_0 . The explicit evaluation of $\langle V_1 \rangle$ is rather complicated, since $\langle V_1 \rangle$ depends on many factors such as the beam diameter, the temperature of the sample, the scattering angle, etc. Furthermore, the midpoint of the beam might not exactly coincide with the height of the critical isochore since the height of the midpoint is known with only finite precision.

The results of our numerical analysis for the moments in $\Delta\Gamma/\Gamma_0$ for xenon and CO_2 will now be presented. We first consider the situation in which the midpoint of laser beam coincides with the height at the critical isochore, i.e. $z_0 = z_c$, and Γ^c is calculated from the mode-mode coupling theory. Figure 10 shows the first-, second-, and third-order corrections, viz. $\langle V_1 \rangle$, $\langle V_2 \rangle$, and $\langle V_3 \rangle$ to the decay rate of xenon as a function of scattering angle for $\Delta T = 0.001$ K and a 0.01-cm-diam beam.

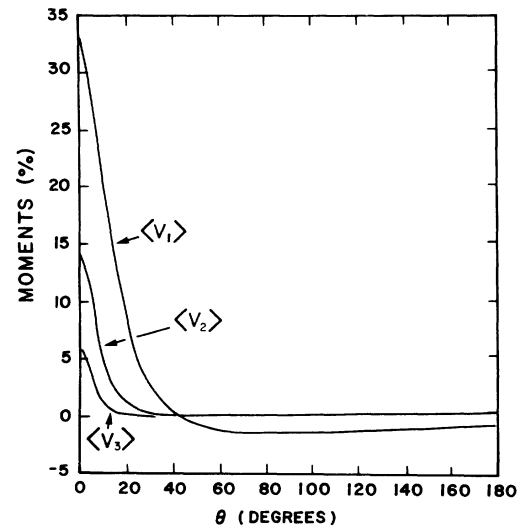


FIG. 10. First three moments in the expansion of the measured time autocorrelation function spatially averaged over a 0.01-cm-diam laser beam for xenon at $\Delta T = 0.001$ K [see Eqs. (18) and (19)] as a function of scattering angle.

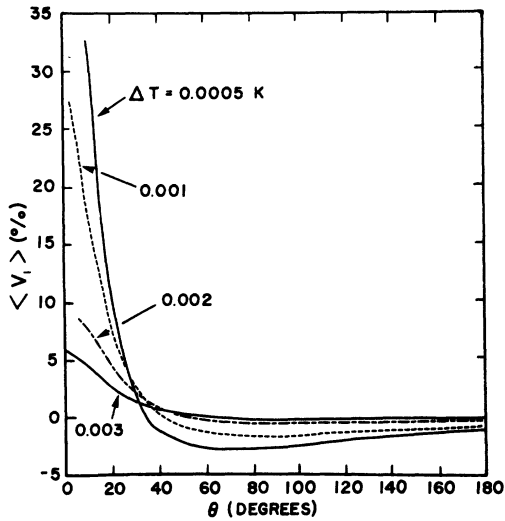


FIG. 11. First-order moment $\langle V_1 \rangle$ for xenon as a function of scattering angle at four temperatures for a 0.01-cm-diam laser beam.

Clearly the main correction comes from the $\langle V_1 \rangle$ term, as anticipated. At very small scattering angles, the moments are quite large and the single exponential approximation [Eq. (20)] will no longer be valid.

Figures 11 and 12 show the first-order moment $\langle V_1 \rangle$ for xenon and CO_2 , respectively as a function of the scattering angle θ at four different temperatures ($0.0005 \leq \Delta T \leq 0.003$ K) and for a 0.01-cm-diam beam. For $\theta \geq 30^\circ$, $\langle V_1 \rangle$ is negative and its magnitude is less than 3% for all temperatures considered here. The reason $\langle V_1 \rangle$ is negative can

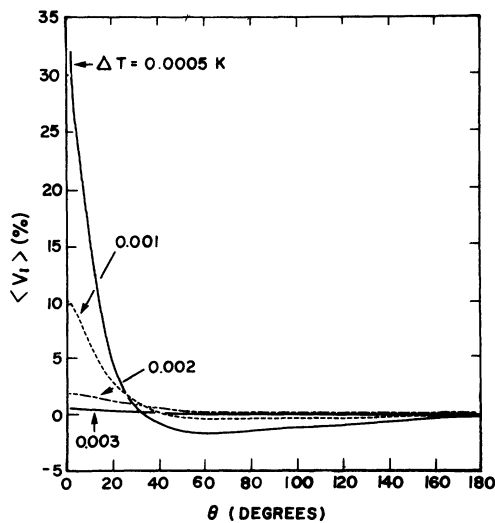


FIG. 12. First-order moment $\langle V_1 \rangle$ for CO_2 as a function of scattering angle at four temperatures for a 0.01-cm-diam laser beam.

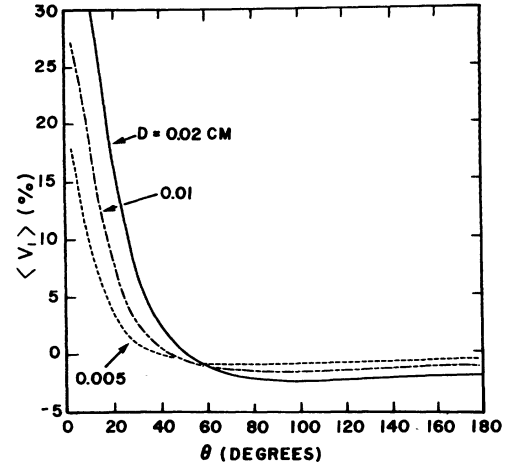


FIG. 13. First-order moment $\langle V_1 \rangle$ for xenon as a function of scattering angle for three beam diameters at $\Delta T = 0.001$ K.

be understood from Fig. 5, which indicates that for these angles and temperatures $\Gamma(z)$ has the maximum value at the center of the beam, i.e. at z_c . This 3% correction due to the spatial averaging effect is less than the uncertainty in currently available experimental data for Γ , which is typically $\pm 5\%$. For $\theta \leq 30^\circ$, $\langle V_1 \rangle$ is positive and strongly dependent on both the scattering angle and the temperature. For instance for xenon at $\theta = 10^\circ$, $\langle V_1 \rangle$ increases from 4.5% at $\Delta T = 0.003$ K to 32% at $\Delta T = 0.0005$ K.

The dependence of $\langle V_1 \rangle$ on the diameter of the laser beam, D , is indicated in Fig. 13, which

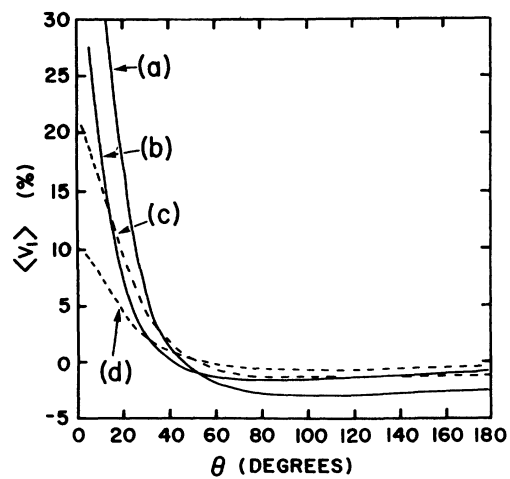


FIG. 14. First-order moment $\langle V_1 \rangle$ for xenon as a function of angle for a 0.01-cm-diam beam. (a) $\Delta T = 0.001$ K and $z_0 - z_c = -0.005$ cm. (b) $\Delta T = 0.001$ K and $z_0 = z_c$. (c) $\Delta T = 0.002$ and $z_0 - z_c = -0.005$ cm. (d) $\Delta T = 0.002$ and $z_0 = z_c$. (z_0 is the midpoint of the laser beam.)

TABLE II. A comparison of values for $\langle V_1 \rangle$ with Γ calculated from the mode-mode coupling and the decoupled-mode theories for CO_2 and Xe at $\Delta T = 0.001$ K with a 0.01-cm-diam beam.

θ (deg)	$\langle V_1 \rangle$ (%) CO_2		$\langle V_1 \rangle$ (%) Xe	
	Decoupled-mode	Mode-mode	Decoupled-mode	Mode-mode
180	0.08	-0.36	0.40	-1.11
135	0.10	-0.41	0.48	-1.27
45	0.67	-0.21	3.04	-0.67
30	1.58	0.69	6.25	2.13
15	4.16	4.06	16.29	11.99
5	9.03	8.95	36.97	27.30

shows $\langle V_1 \rangle$ for xenon as a function of θ at $\Delta T = 0.001$ K for three values of D (0.02, 0.01, and 0.005 cm). The correction at say $\theta = 10^\circ$ ranges from 9% for $D = 0.005$ cm to 31% for $D = 0.02$ cm.

In our discussion thus far, the midpoint of the laser beam has been assumed to coincide with the height of the critical isochore. As the beam center is moved off the critical isochore, the correction relative to the value of Γ at the center of the beam decreases since the density gradient across the beam becomes smaller. In an experiment the decay rate is measured as a function of z , and the minimum in Γ is taken to be the value at the critical density. However, because of the finite resolution of the sample height (typically ± 0.01 cm) the midpoint of the beam might in fact never coincide with z_c . Moreover, as suggested in Fig. 5, the minimum in Γ might not occur at $z = z_c$. Consequently, the correction relative to the theoretical value of Γ at the critical isochore must also be considered for $z_0 - z_c \leq \delta h$, where δh is the experimental uncertainty in the measurement of z .

Figure 14 shows $\langle V_1 \rangle$ for xenon as a function of angle for four cases: (a) $\Delta T = 0.001$ K and $z_0 - z_c = -0.005$ cm, (b) $\Delta T = 0.001$ K and $z_0 - z_c = 0$, (c) $\Delta T = 0.002$ K and $z_0 - z_c = -0.005$ cm, (d) $\Delta T = 0.002$ K and $z_0 - z_c = 0$. In each case the correction is with respect to the value of the decay rate at the critical density, i.e., $\Gamma(\rho_c)$. (The corrections are nearly symmetrical about z_c ; so we do not show the case $\Delta z = 0.05$ mm.) Since the position of the midpoint of the beam relative to z has an assumed uncertainty of ± 0.05 mm, the actual correction will lie somewhere between the values at the two extremes. In the cases shown in Fig. 10, these ranges are 18.3% to 38% at $\Delta T = 0.001$ K and 7.8% to 16% at $\Delta T = 0.002$ K, for a 10° scattering angle.

When the decoupled-mode expression for Γ° is used, the finite-beam effects are qualitatively similar but slightly different in magnitude. Table II compares $\langle V_1 \rangle$ for xenon and CO_2 at $\Delta T = 0.001$ K and for several angles with Γ° calculated from both the mode-mode coupling and the decoupled-mode

theories.

The results of the numerical calculations for typical experimental conditions very near the critical point can be summarized as follows. The finite-beam diameter correction is less than -3% for $30^\circ \leq \theta \leq 180^\circ$, but at smaller angles the correction becomes very large, even at $\Delta T = 0.003$ K. Departures from a single exponential fit for the time-autocorrelation function should become detectable at angles less than 5° .

V. CONCLUSIONS

The effects of gravitationally induced density gradients very near the critical point are summarized as follows: (i) The minimum value of Γ as a function of height in the fluid does not necessarily occur at the critical isochore. (ii) When the mode-mode coupling theory of critical-point dynamics is used to calculate the decay rate, $\Gamma(z)$ has a minimum significantly different from $\Gamma(z_c)$ at a height slightly lower than the height of the critical isochore. (iii) The decoupled-mode theory also predicts a minimum in $\Gamma(z)$ away from z_c , but the departure from $\Gamma(z_c)$ is quite small. (iv) At small scattering angles the measured decay rate, which represents a value spatially averaged over the intensity profile of the laser beam, can be significantly different from Γ at the midpoint of the beam.

Conclusions (i), (ii), and (iii) result directly from the increase in Γ as a function of $q\xi$ for $q\xi > 3$, which is rather significant for the mode-mode coupling theory and can give rise to negative values of the first-order moment $\langle V_1 \rangle$. This appreciable upward trend in $\Gamma(q\xi)$ for the mode-mode coupling theory is due primarily to the factor $R(q\xi)$ which appears in Eq. (9a) and which incorporates various refinements to the theory.

Experimental light-scattering data currently available do not cover the regions in angle and temperature in which these effects should be observable. The major limitation on the quantitative

measurements of these density-gradient effects is temperature control; the sample temperature must be maintained to within much less than 0.001 K. Photon autocorrelation spectroscopy provides the necessary precision for measuring the decay rate of the scattered-field time autocorrelation function, and a focused beam diameter small enough to minimize the spatial-averaging effects can be achieved. Precise measurements of Γ as a function of height very close to the critical point will

provide a sensitive test of the two theories of critical-point dynamics.

Our analysis is being extended to the case of a binary mixture. For a mixture, the thermodynamic derivative $(\partial\rho/\partial P)_{T,\mu}$, which corresponds to K_T for a pure fluid, is strongly divergent at the critical mixing point.¹⁸ Consequently, an anomalous density and concentration gradient should also appear in the mixture.

*Work supported in part by National Science Foundation.

¹R. Mountain, *Rev. Mod. Phys.* **38**, 205 (1966).

²H. L. Swinney and D. L. Henry, *Phys. Rev. A* **8**, 2586 (1973).

³K. Kawasaki, *Phys. Lett. A* **30**, 325 (1969); *Ann. Phys. (N.Y.)* **61**, 1 (1970); *Phys. Rev. A* **1**, 1750 (1970).

⁴S. M. Lo and K. Kawasaki, *Phys. Rev. A* **8**, 2176 (1973).

⁵K. Kawasaki and S. M. Lo, *Phys. Rev. Lett.* **29**, 48 (1972).

⁶R. A. Ferrell, *Phys. Rev. Lett.* **24**, 1169 (1970).

⁷R. Perl and R. A. Ferrell, *Phys. Rev. Lett.* **29**, 51 (1972); *Phys. Rev. A* **6**, 2358 (1972).

⁸L. Van Hove, *Phys. Rev.* **95**, 1374 (1954).

⁹Ornstein and Zernike, *Proc. Acad. Sci. Amst.* **17**, 793 (1914); *Z. Phys.* **19**, 134 (1918).

¹⁰See, e.g., P. A. Egelstaff, *An Introduction to the Liquid State* (Academic, N.Y. 1967).

¹¹P. Schofield, *Phys. Rev. Lett.* **22**, 606 (1969).

¹²J. T. Ho and J. D. Litster, *Phys. Rev. Lett.* **22**, 603 (1969).

¹³C. C. Huang and J. T. Ho, *Phys. Rev. A* **7**, 1304 (1973).

¹⁴J. V. Sengers and P. H. Keyes, *Phys. Rev. Lett.* **26**, 70 (1971).

¹⁵P. C. Hohenberg and M. Barmatz, *Phys. Rev. A* **6**, 289 (1972).

¹⁶T. K. Lim, Ph.D. thesis (Johns Hopkins University, 1973) (unpublished).

¹⁷K. J. Czworniak and D. R. Jones, *J. Opt. Soc. Am.* **64**, 86 (1974).

¹⁸L. Mistura, *J. Chem. Phys.* **55**, 2375 (1971).